Luminescence study of KLuP$_2$O$_7$ doped with Pr^{3+} ions under different types of excitation

S. A. Kiselev and V. A. Pustovarov

🌐
View Online

⬆
Export Citation

ARTICLES YOU MAY BE INTERESTED IN

Luminescence Study of $KLuP_2O_7$ Doped with Pr^{3+} Ions under Different Types of Excitation

S. A. Kiselev[a) and V. A. Pustovarov

Institute of Physics and Technology, Ural Federal University, 19 Mira st., Ekaterinburg, 620002, Russia

a)Corresponding author: sviat-kiselev@yandex.ru

Abstract. This paper reports the spectroscopic properties of praseodymium-doped potassium lutetium double phosphates, $KLuP_2O_7$:Pr^{3+}(1%). Spectra of photoluminescence (PL), PL excitation, X-ray excited luminescence and pulse cathodoluminescence, thermally stimulated luminescence were measured. $KLuP_2O_7$:Pr^{3+} showed Pr^{3+} emission connected both with high intensity interconfigurational $4f^{1}5d^{1} \rightarrow 4f^{2}$ transitions (UV bands in region of 250-320 nm), intraconfigurational $4f^{2} \rightarrow 4f^{2}$ transitions (weak lines in vision spectral region) and Stocks defect-related luminescence. Upon both UV intra-center and band-to-band excitation with ionizing radiation, emission spectra of $KLuP_2O_7$:Pr^{3+} are dominated by Pr^{3+} interconfigurational $4f^{1}5d^{1} \rightarrow 4f^{2}$ radiative transitions. Luminescence decay kinetics measurements established decay time $\tau \approx 19$ ns at room temperature. The study of thermally stimulated luminescence demonstrates effective light storage. Parameters of charge carriers' traps were calculated: $\Delta E_1 = 1.1$ eV (for peak at 352 K) and $\Delta E_2 = 1.3$ eV (for peak at 388 K).

INTRODUCTION

Praseodymium-ions doped luminescent materials are recently being actively investigated due to demonstration of fast interconfigurational $5d - 4f$ optical transitions. Pr^{3+}-doped hosts are doubly demanded in systems working at higher count rate – they are characterized with short wavelengths and fast decay time [1]. Such systems one can face up in different spheres such as nuclear physics, security, chemistry, space physics, medical imaging, etc. The application of such materials is rather perspective in medical and detectors fields. Many detecting materials are doped with Ce^{3+} ions. Praseodymium emission in comparison with cerium ions is located in higher energy region and is characterized with shorter lifetime (about 17 instead of 30 ns) [2, 3]. The search of new scintillating materials is very actual problem of modern investigation researches. The study of $KLuP_2O_7$ doped with Pr^{3+} was started in Refs. [4, 5]. $KLuP_2O_7$ with Ce^{3+} and Pr^{3+} is one of the most promising materials among fast energy converters transformers. Previous researchers have proposed application potential of this material based on VUV-spectroscopy data only (emission and excitation spectra, its decay kinetic measurement).

OBJECT AND EXPERIMENTAL DETAILS

Powder microcrystalline material with a stoichiometry of $KLu_{0.99}Pr_{0.01}P_2O_7$ (*i.e.* containing 1 mol.% Pr^{3+} substituting for Lu^{3+}) were obtained by solid-state reaction at Laboratory of Luminescent Materials, University of Verona. The constituent high purity raw materials KNO_3, $(NH_4)_2HPO_4$, Lu_2O_3, and Pr_6O_{11} (the last two reagents 4N) were mixed and heat treated in a horizontal furnace in air for 1 h at 400 ºC and 24 h at 750 ºC with intermediate regrinding. The flowchart of powder synthesis is presented in Fig. 1 The phase purity of the prepared sample was examined using powder X-ray diffraction (PXRD) technique with a Thermo ARL X'TRA powder diffractometer, operating in the Bragg-Brentano geometry and equipped with a Cu anode X-ray source (K_α, $\lambda = 1.5418$ Å) with a Peltier Si(Li) cooled solid-state detector. The obtained PXRD pattern was fully compatible with ICDD Card No. 01-076-7386 and with the previous results documented in Ref. [4]. It is worth reminding here, that this material

crystallizes in a monoclinic structure belonging to space group $P2_1/c$ (no. 14) [6]. The crystal structure of $KLuP_2O_7$ offers only one site for Lu^{3+} (or Pr^{3+}) with a coordination number of 6 and point symmetry C_1.

The experimental results presented in this paper were obtained applying different techniques. Photoluminescence (PL) and PL excitation spectra upon excitation in the UV energy range (from 3.5 to 5.8 eV) were measured at the Laboratory of Solid State Physics, Ural Federal University. To excite the luminescence a 400 W deuterium lamp and a LOMO DMR-4 primary prismatic double monochromator were used. A secondary DMR-4 monochromator equipped with a Hamamatsu R6358-10 photomultiplier (PMT) was used to detect the emission signal. The X-ray excited studies performed at the same laboratory included measurements thermally stimulated luminescence (TSL) glow curves. The luminescence was detected using a LOMO MDR-23 monochromator and a FEU-106 PMT. A BSV-2 X-ray tube (30 kV, 10 mA, Cu anode) was used for excitation. TSL glow curves were measured in the range of 90 – 610 K after X-ray irradiation at T= 90 or 295 K with a heating rate of 0.33 K/s.

The measurements of decay kinetics and emission spectra upon excitation with non-monochromatic X-ray synchrotron radiation (E = 3–60 keV, pulse FWHM ~ 1 ns, frequency ~ 8 MHz) were performed at the beamline #6 of the VEPP-3 storage ring at Budker Institute of Nuclear Physics (Russia). Stroboscopic method of electron-optical chronography with sub-nanosecond time resolution was used. The detection system included a SOL Instruments MS2004 monochromator equipped with a high-speed LI-602 dissector [7].
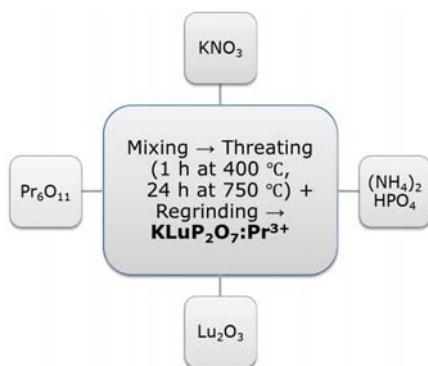

FIGURE 1. Flowchart of powder synthesis

The pulse cathodoluminescence (PCL) spectra and PCL decay kinetics were measured using Radan-330A pulse electron gun (E = 120 keV, pulse FWHM = 200 ps, rate 5 Hz) at University of Tartu (Estonia). A 0.3 m Andor Shamrock 303i monochromator equipped with a MCP-PMT detector was used for the registration [8].

All emission spectra were corrected for the spectral sensitivity of the detection systems. PL excitation spectra were corrected for wavelength dependent photon flux variation using yellow lumogen.

RESULTS AND DISCUSSION

UV Photoluminescent Spectroscopy

Photoluminescence (PL) (Fig. 2, a) and PL excitation (Fig. 2, b) spectra were measured at room temperature in the laboratory of Solid state physics, UrFU. Stokes PL spectra at different energies of exciting photons as well pulse cathode luminescence (PCL) spectra (Fig. 4) contain a set of wide bands and lines corresponding to radiative transitions in the Pr^{3+} ions as well as defect-related luminescence band. All radiation transitions and electron states of the Pr^{3+} ions were determined using Dike's energy diagram for Pr^{3+} ion (Fig. 3) [2].

With excitation of 5.3 or 5.5 eV photons the broad emission bands with maxima at 248 and 285 nm are dominating. They correspond to the parity-allowed interconfigurational radiative transitions from the lowest excited $4f^15d^1$ state to the multiplets of the ground $4f^2$ electronic configuration of the Pr^{3+} ion. A broad shoulder in 430 nm region is supposed to present the defect-related luminescence. More obviously this luminescence with maximum near 450 nm is demonstrated under excitation of 5.0 eV photons.

PL excitation spectra were measured for the main emission bands of $d - f$ and defect-related luminescence. According to energy scheme of Pr^{3+} ions presented in Fig. 3 [2], it can be understood that we are working with the middle situation, when $4f^15d$ energy band is lower than $^1S_0$ level. As it can be concluded from PL and PL excitation

spectra, there are two dominant channels of emission: besides $d-f$ transitions active defect-related luminescence is a serious competitive channel of capturing charge carries. The contribution of $4f^2 \rightarrow 4f^2$ is very low due to a small Stokes shift. In according with [9], with Stokes shift less than 0.4 eV, the contribution of interconfigurational $d-f$ emission will dominate over intraconfigurational $f-f$ transitions. As it can be observed from PL spectra, the Stokes shift of $d-f$ emission does not exceed 0.38 eV, so we can observe domination of interconfigurational transitions.

(a)

(b)
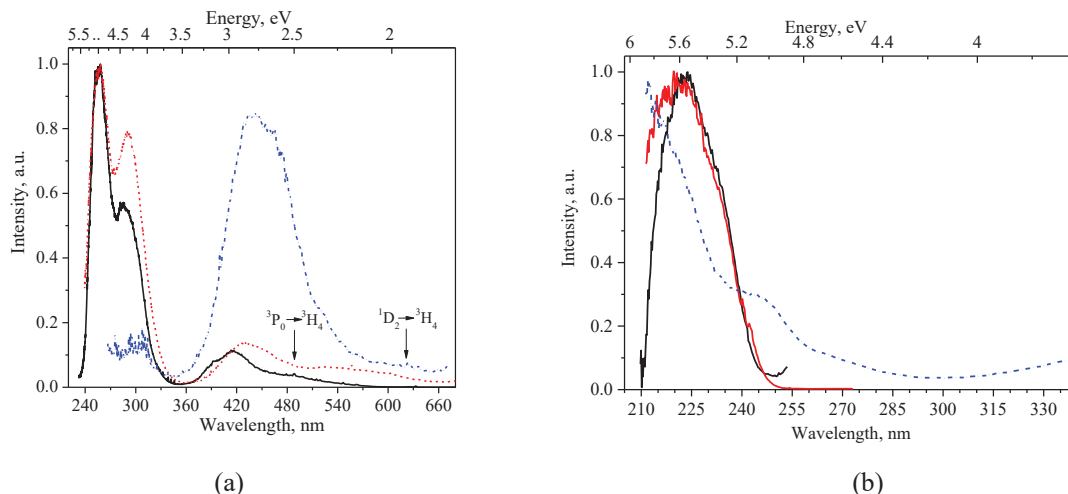
FIGURE 2. (a): Photoluminescence spectra of $KLuP_2O_7$:Pr^{3+} upon different excitation energy E_{exc}: 5.0 eV (blue), 5.3 eV (red), 5.5 eV (black), T=295 K. (b): PL excitation spectra of $KLuP_2O_7$:Pr^{3+} of different emission energy E_{emis}: 2.8 eV (blue), 4.1 eV (red), 4.62 eV (black), T = 295 K
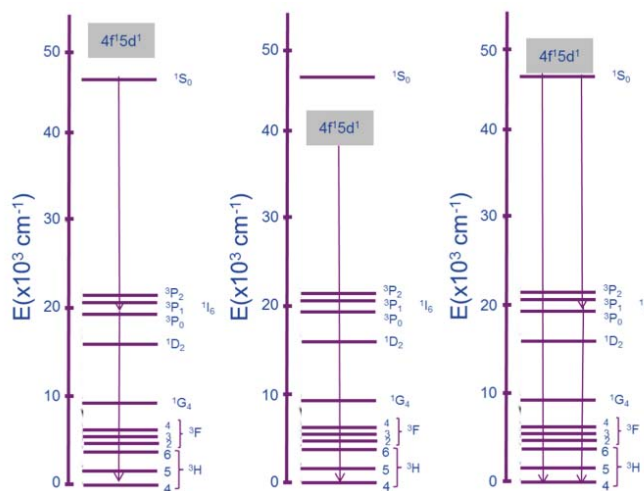

FIGURE 3. Energy level scheme of electron states in Pr^{3+} ion. Three options for the position of the $4f^1 5d$ configuration zone relative to $^1S_0$ level are shown [2]

Pulse Cathode Luminescence Spectroscopy

Figure 4 shows time-resolved PCL spectra measured at T= 295 K. The spectra were taken within two independent time windows (TW) which collect the emission signal in time windows of 0-32 ns ('fast' TW) and 0-2 ms ('slow' TW) after the excitation cathode ray shot. The spectrum taken in "fast" TW shows the presence of fast $4f^1 5d^1 \rightarrow 4f^2$ emission. Spectrum measured in 'slow' TW demonstrates not only interconfigurational transitions, but also trends of defect- related and $4f^2 \rightarrow 4f^2$ weak transitions. These are 490 and 612 nm lines that can be observed only

by closer examination. It should be noticed that interconfigurational bands correlate perfectly with PL spectra presented above.
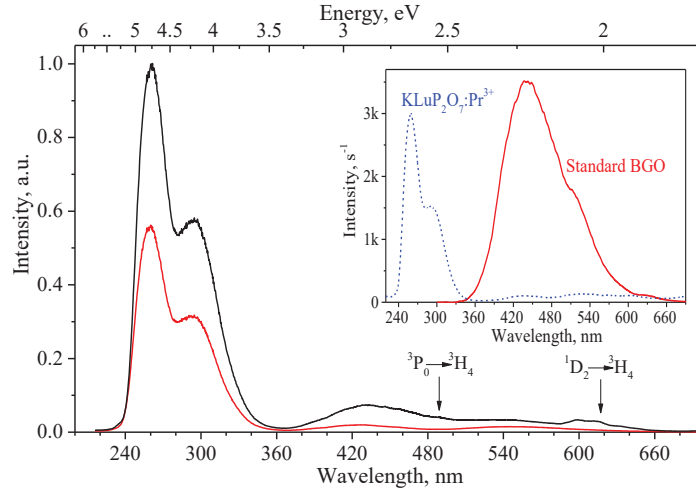
FIGURE 4. PCL spectra of KLuP$_2$O$_7$:Pr^{3+} recorded in slow (black) and fast (red) time windows, T = 295 K. Inset: Comparison of light output of KLuP$_2$O$_7$:Pr^{3+} and BGO powder measured in identical conditions at T 295 K

Inset shows the comparison of light output of KLuP$_2$O$_7$ and standard BGO powder measured in identical conditions. Integral area under operating region of our powder contains about 40 % of BGO output. It has to be said that operating area of BGO powder is in 300-700 nm region, it is the area of self-trapped excitons emission. The area of KLuP$_2$O$_7$:Pr^{3+} is located in the range of $4f^15d^1 \rightarrow 4f^2$ transitions (240 – 360 nm). We observe the relative output in terms of working with powders, what complicates the measurement of absolute light output. But it must be mentioned, that in [10] the absolute output of BGO is given as 8500 Photons/MeV.

Luminescence Decay Kinetics

Decay kinetics of 260 nm line of interconfigurational $d - f$ luminescence excited with cathode ray shot and synchrotron X-rays are presented in Fig. 5 (a) and 5 (b), respectively. Luminescence decay kinetics upon X-ray excitation can be described with mono-exponential behaviour with the lifetime of 18.4 ns. PCL decay kinetics of UV-emission bands (f. e. 260 nm) shows no build-up stage; this indicates a prompt population of the Pr^{3+} $4f^15d^1$ levels by host electronic excitations, which is a typically beneficial result of recombinational mechanism of energy transfer. It can be well fitted with two-exponential approximation

$$I(t) = A_1 \cdot \exp(-t/\tau_1) + A_2 \cdot \exp(-t/\tau_2) + I_0, \qquad (1)$$

where A_i are weight coefficients and τ_i are lifetimes of decay components, the parameter I_0 is a luminescence intensity at longer times and it characterizes the contribution of slow components. Obtained parameters of lifetimes are 20.0 ns for fast and 75 ns for slow component. The contribution of the slow components is less than 10^{-4}. Kinetics lifetimes for X-ray and cathode ray excitation are close in value, what indicates that electron-hole recombination in Pr^{3+} ion does not delay the immediate population of Pr^{3+} $4f^15d^1$ excited state.

The PCL decay kinetics recorded for 430 nm line of defect-related luminescence (Fig. 5, b) demonstrate different behaviour. It can be also well fitted with two-exponential approximation, but in contrary, there is a well-observed built-up stage characterized with rise time of 4.8 ns. Obtained decay times of this kinetics are 22.5 ns for fast component and 2.65 μs for slow component. The build-up stage may indicate the presence of shallow traps which act as intermediate trapping centers for thermalized charge carriers, this is approved in thermally stimulated luminescence measurements.
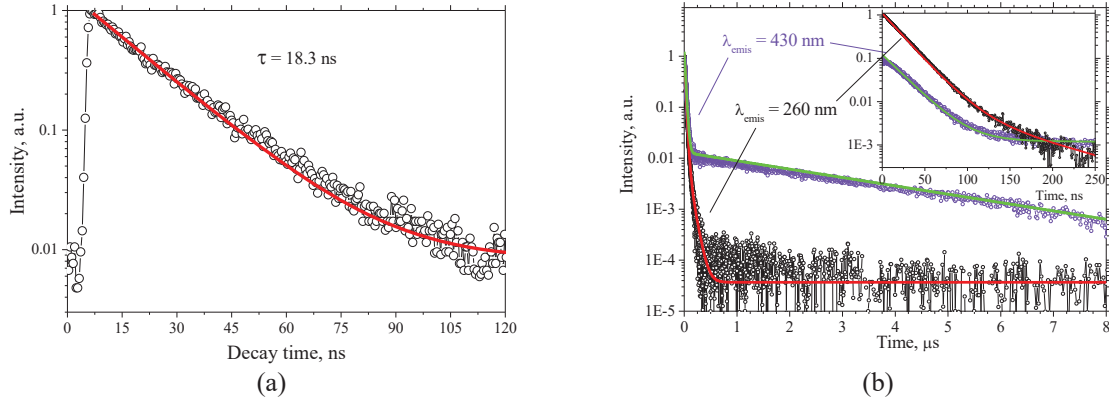
FIGURE 5. (a): Decay kinetics recorded monitoring the Pr^{3+} $4f^{1}5d^{1}{\rightarrow}4f^{2}$ emission (260 nm, black mads) in $KLuP_2O_7$:Pr^{3+} upon excitation with high frequency X-ray synchrotron radiation, T = 295 K and approximating curve (red). (b): Decay kinetics recorded monitoring Pr^{3+} $4f^{1}5d^{1}{\rightarrow}4f^{2}$ emission (260 nm, black mads) with approximation (red) and defect-related emission (430 nm, purple mads) with approximation curve (green) in $KLuP_2O_7$:Pr^{3+} upon cathode ray excitation in μs scale and ns scale (Inset), T = 295 K

Thermoluminescent Measurements

The study of thermally stimulated luminescence (Fig. 6) demonstrates effective light storage. TL afterglow was approximated by the means of built-in Origin 9.0 instrument of peak detection. A special function based on [11] expressions was applied. Approximating function can manifest the parameters of every peak's curve via calculating of analytic expressions (2) and (3):

$$I(T) = I_m \cdot b^{b/(b-1)} \cdot \exp\left(\frac{E}{kT} \cdot \frac{T-T_m}{T_m}\right) \cdot \left[(b-1) \cdot (1-\Delta) \cdot \frac{T^2}{T_m^2} \cdot \exp\left(\frac{E}{kT} \cdot \frac{T-T_m}{T_m}\right) + Z_m\right]^{-b/(b-1)}; \qquad (2)$$

$$s = \frac{\beta E}{kT_m^2} \cdot \frac{1}{Z_m} \exp\left(\frac{E}{kT_m}\right). \qquad (3)$$

Here, $I(T)$ means TSL intensity with maximum of I_m, b is kinetics order, E – energy trap depth, T_m – temperature of peak's maximum, $\Delta = 2kT/E$, $\Delta_m = 2kT_m/E$, $Z_m = 1+(b-1)\Delta_m$. In equation (3), s is a frequency factor, β is the heating rate. Each peak is calculated separately, and summarizing of approximating curves presents the original spectrum. According to obtained by approximation process parameters we are able to get the information about electron traps' energy depth and numerical meaning of frequency factor. Approximating process allows to identify two energy traps characterized with kinetics order b = 2. Activation energy of the first peak (T_{max} = 352 K) consists ΔE = 1.1 eV with frequency factor s = 2.7·10^{13} s^{-1}. The second peak with maximum at T= 388 K has parameters: ΔE = 1.3 eV and s = 1.4·10^{16} s^{-1}.

TSL spectra prove the presence of defect-related traps, where the recombination of charge carriers takes place. The features of recombination luminescence proved with TSL studies signify the presence of defects in the crystal structure. From the results of PL studies, it can be easily observed that energy transfer from the impurity center to the defects. This means that efficient output of recombination energy transfer from the host to Pr^{3+} impurity centers is limited and the competitive charge carriers capturing channel by the host defects exists.

CONCLUSION

To summarize, $KLuP_2O_7$:Pr^{3+} powder was synthesized via solid state reaction. A complex of various techniques was applied to observe optical properties of this sample. Upon both UV intra-center and band-to-band excitation with X-ray or cathode beam, the emission spectra are dominated by praseodymium interconfigurational $f - d$ radiative transitions. These transitions are dominating in spectra (both PL and PCL), but besides, a contribution of defect-related luminescence is observed. Decay kinetics measurements established decay time about 19 ns. Exited with cathode ray shot, they have no built-up stage, what indicates a prompt population of the Pr^{3+} $4f^{1}5d^{1}$ levels by host electronic excitations. Meanwhile, the delayed energy transfer was suggested to originate from re-trapping of

charge carriers at defect-related traps whose presence was demonstrated with thermoluminescent measurements. The relative output of $KLuP_2O_7:Pr^{3+}$ in comparison with BGO powder is rather high, what, in addition to perfect timing features of this compound can be regarded as recommendation for future application in fast detecting systems.
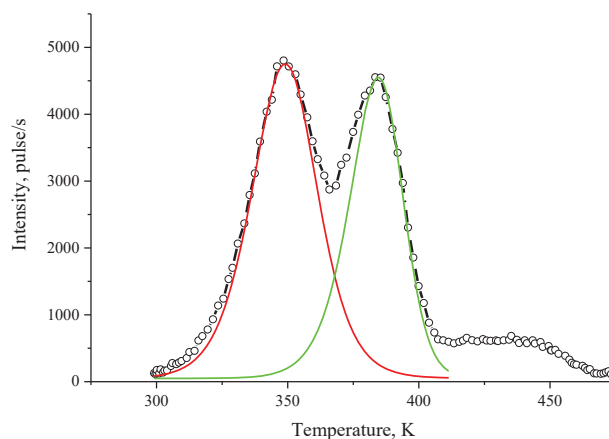
FIGURE 6. TL afterglow (black mads) and approximating curves (red, green) of X-ray irradiated at T = 295 K $KLuP_2O_7:Pr^{3+}$

ACKNOWLEDGMENTS

REFERENCES

1. M. Nikl, V.V. Laguta, A. Vedda, Phys. Status Solidi (b) **245**, 1701-1722 (2008),
2. A.M. Srivastava, J. Lumin. **169**, 445-449 (2016).
3. A. Zych, M. de Lange, C. d. M. Donega, A. Meijerink, J. Appl. Phys. **112**, 013536 (2012).
4. M. Trevisani, K. Ivanovskikh, F. Piccinelli, M. Bettinelli, J. Chem. Sci. **69**, 205-209 (2014).
5. J.L. Yuan, X.J. Wang, D.B. Xiong, C.J. Duan, J.T. Zhao, Y.B. Fu, G.B. Zhang, C.S. Shi, J. Lumin. **126**, 130-134 (2007).
6. S.I. Omelkov, V. Nagirnyi, E. Feldbach, R. M. Turtos, E. Auffray, M. Kirm, P. Lecoq, J. Lumin. **191 A**, 61-67 (2017).
7. V.A. Pustovarov, E.I. Zinin, A.L. Krymov, B.V. Shulgin, Rev. Sci. Instrum. **63**, 3521 (1992).
8. J.-L. Yuan, H. Zhang, H.-H. Chen, X.-X. Yang, J.-T. Zhao, M. Gu, J. Solid State Chem. **180**, 3381-3387 (2007).
9. D. Wisniewski, L.A. Boatner, IEEE Trans. Nucl. Sci. **56**, 3806-3818 (2009).
10. M. Moszynski, M. Kapusta, M. Mayhugh, D. Wolski, S.O. Flyckt, IEEE Trans. Nucl. Sci. **44**, 1052-1061 (1997).
11. G. Kitis, J. M. Gomez-Ros and J. W. N. Tuyn, J. Phys. D: Appl. Phys. **31**, 2636–2641 (1998).